Materials and Design 165 (2019) 107566

Contents lists available at ScienceDirect

Materials and Design

journal homepage: www.elsevier.com/locate/matdes

Polysaccharide hydrogels for multiscale 3D printing of pullulan scaffolds

Gioia Della Giustina [a,b,1], Alessandro Gandin [a,b,c,1], Laura Brigo [a,b], Tito Panciera [c], Stefano Giulitti [c], Paolo Sgarbossa [a,b], Delfo D'Alessandro [d], Luisa Trombi [d], Serena Danti [e], Giovanna Brusatin [a,b,*]

[a] Department of Industrial Engineering, University of Padova, Via Marzolo 9, 35131 Padova, Italy
[b] INSTM, Padova Research Unit, Via Marzolo 9, 35131 Padova, Italy
[c] Department of Molecular Medicine, University of Padova, via Ugo Bassi 58/B, 35131 Padova, Italy
[d] Department of Surgical, Medical, Molecular Pathology and Emergency Medicine, University of Pisa, via Savi 10, 56126 Pisa, Italy
[e] Department of Civil and Industrial Engineering, University of Pisa, Largo L. Lazzarino 2, 56122 Pisa, Italy

HIGHLIGHTS

- Fabrication of hydrogels scaffolds made of methacrylathed pullulan.
- Multiscale light assisted 3D printing (visible stereolithography and two-photon lithography).
- Functionalization of pullulan based scaffolds with extracellular matrix proteins
- Demonstration that, after functionalization, the scaffolds support adhesion and growth of ephitelial and mesenchymal cells

GRAPHICAL ABSTRACT

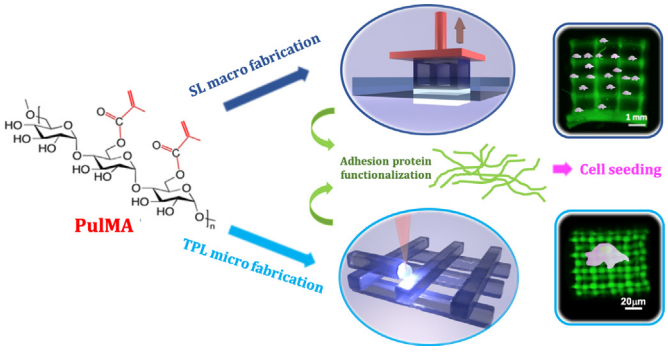

ARTICLE INFO

Article history:
Received 22 November 2018
Received in revised form 21 December 2018
Accepted 22 December 2018
Available online 2 January 2019

Keywords:
Hydrogel
Biomaterials
Polysaccharide
Pullulan
3D printing
Two photon laser lithography
Mesenchymal stromal cells

ABSTRACT

Structurally and mechanically similar to the extracellular matrix (ECM), biomimetic hydrogels offer a number of opportunities in medical applications. However, the generation of synthetic microenvironments that simulate the effects of natural tissue niches on cell growth and differentiation requires new methods to control hydrogel feature resolution, biofunctionalization and mechanical properties. Here we show how these goals can be achieved by using a pullulan-based hydrogel, engineered in composition and server as cell-adhesive hydrogel, 3D photo-printable in dimension, ranging from the macro- to the micro-scale dimensions, and of tunable mechanical properties. For this, we used absorbers that limit light penetration, achieving 3D patterning through stereolithography with feature vertical resolution of 200 μm and with overall dimension up to several millimeters. Furthermore, we report the fabrication of 3D pullulan-modified hydrogels by two-photon lithography, with sub-millimetric dimensions and minimum feature sizes down to some microns. These materials open the possibility to produce multiscale printed scaffolds that here we demonstrate to be inert for cell adhesion, but biologically compatible and easily functionalizable with cell adhesive proteins. Under these conditions, successful cell cultures were established in 2D and 3D.

1. Introduction

Tissue engineering and regenerative medicine ultimately rely on the development of accurate replica of natural tissues and native 3D cell

* Corresponding author at: Department of Industrial Engineering, University of Padova, Italy.
E-mail address: giovanna.brusatin@unipd.it (G. Brusatin).
[1] These authors contributed equally.

https://doi.org/10.1016/j.matdes.2018.107566

environments in terms of multiscale architecture, composition, biochemical properties and physical characteristics [1,2]. In this context, biocompatible materials must be engineered to recapitulate the mechanical features of natural extracellular matrix (ECM), and to precisely reproduce morphological and architectural aspects in a broad range of dimensions across multiple scales (from millimeter to micron). For this challenge, hydrogels, either synthetic, such as polyacrylamide and polyethylene glycol (PEG), or natural, such as gelatin and hyaluronic acid, have emerged as technologically pliable, multifunctional and cell-compatible materials [3–5]. At the same time, printing procedures able to impart complex 3D architectural features to hydrogel scaffolds remain in their infancy [6–10].

Pullulan is a non-ionic linear polysaccharide, naturally produced from starch by *Aureobasidium pullulans*, consisting of maltotriose units connected by $\alpha(1 \rightarrow 4)$ glycosidic bond, consecutively linked to each other by $\alpha(1 \rightarrow 6)$ glycosidic linkages. Among natural polysaccharides, it has many advantageous properties: it's biodegradable, edible, bio- and blood-compatible, non-toxic, non-immunogenic, non-mutagenic and non-carcinogenic [11,12]. Moreover, it is easily soluble in water allowing a clear and viscous hydrogel to be prepared. Pullulan has been proposed as anti-adhesive barrier layer for the prevention of post-operative problems [13,14] and is biocompatible and FDA approved (widely used in cosmetics [15]). Thanks to its free-radical quenching ability, it has been also used in form of nanofibers or coatings for food preservation [16] and more recently for application in tissue engineering and regenerative medicine [11,12,17–20]. For example, pullulan composite matrices loaded with nano-hydroxyapatite fillers for bone tissue engineering have been successfully reported and were able to stimulate production of bone proteins both in vitro and in vivo, showing potential to regenerate bone defects [21]. Therefore, thanks to its biodegradability [11,12], it's use in tissue engineering is potentially attractive.

We reasoned that pullulan could be custom modified on its hydroxyl groups with desired chemical moieties (for example chemical polymerizable groups) in order to generate 3D crosslinked structures of tunable mechanical properties. Indeed, in spite of these attractive chemical features, the potential of pullulan for the generation of scaffolds or culture systems with specific 2D and 3D shapes and morphologies has so far remained unexplored.

In this work, we synthesized methacrylated pullulan (PulMA) hydrogels that have been printed by multiscale light assisted 3D printing techniques. By using visible stereolithography apparatus (SL) and two-photon lithography (TPL), we produced 3D patterns from millimeters down to few microns as well as suspended structures. Using further engineering the material into a photosensitive formulation, we built complex 3D shapes through spatially controlled irradiation (SL), overcoming current limitations in structuring along the third dimension [22].

Mechanical properties, in particular rigidity, were controlled by the addition of a bifunctional crosslinker that enabled to tune elastic modulus and water absorption of PulMA hydrogels. Finally, cell lines and mesenchymal stem cells (MSCs) were seeded both on macro- and micrometric 3D structures, to test biological response, as such validating pullulan as new and attractive biomaterial substrate for cell biological and, in perspective, regenerative medicine applications.

2. Materials and methods

2.1. Materials

Pullulan (Mw 200,000) was obtained from SinoBIO. Polyethyleneglycoldiacrylate (PEGDA Mn 575), methacrylic anhydride 94% (MA), 3-(trimethoxysilyl)propyl methacrylate 98% (TMSPM) and dimethylsulfoxide 99.9% (DMSO) were purchased from Sigma-Aldrich and used without further purification. Bis(2,4,6-trimethylbenzoyl)-phenylphosphineoxide (IRGACURE 819) and 2-hydroxy-4-(2-hydroxyethoxy)-2-methylpropiophenone (IRGACURE 2959), kindly provided by BASF, were used as radical photoinitiator for visible stereolithography and UV polymerization tests, respectively. A non-commercial water-soluble two-photon initiator [23], benzylidene cycloketone-based (P2CK), was used as initiator for two-photon polymerization (2PP).

For cell culture and analysis, the following reagents and supplies were purchased: Density gradient Ficoll-Paque Plus from GE Healthcare, Hatfield, UK; T-75 tissue culture flasks and 6-well plates from Sarsted, Numbrecht, Germany; Dulbecco's Modified Eagle Medium – Low Glucose (DMEM-LG), Fetal Bovine Serum (FBS), L-glutamine, Penicillin-Streptomycin (PEN-STREP) solution, alamarBlue®, LIVE/DEAD® cell viability assay, Alexa Fluor 488 phalloidin and 4′,6-diamidino-2-phenylindole (DAPI) from Thermo Fisher Scientific, Waltham, MA, USA; fluconazole from Fresenius Kabi, Verona, Italy; Trypan Blue staining, gelatin (type B from bovine skin, 75 Bloom), trypsin, Phosphate Buffered Saline (PBS), hematoxylin, eosin, and Fluoromount mountant medium from Sigma-Aldrich Milan, Italy; neutral buffered formalin, and Killik from Bio-Optica, Milan, Italy; calcium chloride solution from Bioindustria Farmaceutici s.r.l., Labaro, Rome, Italy; ApoAlert® Annexin V Apoptosis kit from Clontech Laboratories, Inc., Mountain View, CA, USA.

2.2. PulMa synthesis and hydrogel formulation

PulMA was synthesized as previously reported [29]. Shortly, pullulan was added to distilled water (2.5% w/v concentration) and stirred at room temperature (RT) until complete dissolution occurred. Solution was cooled down to 4 °C and MA was slowly added up to a concentration of 0.5% v/v. The reaction was stirred for 24 h at 4 °C, keeping the pH at 8 by means of NaOH 10 M additions.

Solution was transparent for all the synthesis time. The product was freeze dried and dialyzed with a dialysis cellulose membrane (molecular weight cut-off, Mw-CO 6000–8000 Da) against warm water at 40 °C for 48 h to remove residual salts and MA. Finally, the solution was lyophilized for 1 day to generate a white porous solid and stored at 4 °C. A degree of functionalization of 3.38% was determined by ^{1}H NMR spectroscopy, as reported in the supporting information.

A 10% w/w solution of PulMA was prepared in distilled H_2O or DMSO. Different weight percentages of PEGDA (10–50% w) with respect to PulMA were added to the sol to modulate the hydrogel mechanical properties and increase crosslinking during 3D fabrication.

In the case of hydrogel solutions for SL, DMSO was used as solvent to dissolve IRGACURE 819 (completely insoluble in water). This commercial photoinitiator was added to the solution to promote the (meth) acrylic units polymerization (5% w with respect to PulMA and PEGDA), through radical mechanism. In water-based solutions, IRGACURE 2959 was employed. Moreover, in order to limit the visible light penetration and improve the z-resolution of the printed structures, the food colorant E133 was used as light absorber. The latter is not present in hydrogel solution for TPL. P2CK was used as initiator for 2PP with a concentration of 1% w/v [23].

2.3. Water absorption and stiffness characterization

To determine the influence of hydrogel formulation on water absorption, that in turn is related to swelling behaviour, a set of samples with different concentrations of light absorber (from 0 to 5% w/w with respect to PulMA + PEGDA) and crosslinker (from 0 to 50% w/w with respect to PulMA) were prepared. Hydrogel solutions (all with a final concentration of 10% w) were deposited on glass coverslips or plastic Petri dishes and exposed to visible light using the DLP source to exactly reproduce the SL printing conditions. A silicone gasket was used to control the hydrogel thickness (approximatively 0.8–1.0 mm) and the coated area ($\phi = 0.5$ cm). To calculate the percentage of water absorption, defined as the fractional increase in the hydrogel weight due to

water absorption, the following equation was used:

$$Water\ absorption\% = \frac{Ws - Wd}{Wd} \cdot 100\%$$

where *Ws* and *Wd* represent the weight of fully hydrated hydrogel after 24–48 h of swelling in distilled H_2O, and the weight of dried hydrogel after swelling and vacuum desiccation for 24 h, respectively.

Hydrogel stiffness as function of PEGDA crosslinker concentration was measured by compressive mechanical tests, performed on samples after 1 night of immersion in water, i.e. in the wet state. PulMA samples in distilled H_2O with 1% of IRGACURE 2959 were UV polymerized and analysed with INSTRON 1121 (Material Testing Machine). Cylindrical shaped discs (10 mm and 3 mm height) immersed in PBS 1× were used for the compression tests. The probe was positioned 1 mm above samples, avoiding any contact before the start of the measurement. A compressive strain rate of 0.5 mm/min was set. The compressive modulus was calculated from the slope of the stress-strain curve in the linear region. A first analysis was performed to evaluate the influence of the concentration of PEGDA Mn 575 in the samples. For all samples the exposure time was 10 s to reproduce SL printing conditions. wt (with respect to PulMA + PEGDA) was used for all samples.

2.4. 3D printing by SL and TPL

Hydrogels containing the proper initiators and a tailored formulation were shaped using two different additive manufacturing 3D printing technologies, SL and TPL. Photocrosslinking of millimetric 3D scaffolds was performed by using a 3D Direct Light Processing (DLP) printer (Robotfactory 3DL Printer-2.0) with a radiation source in the visible range (400–600 nm), slicing between 10 and 1000 μm and a nominal x-y resolution of 50 μm. In addition, an optical bandpass filter was used to narrow the projector emission between 400 and 500 nm and further select the exposure wavelength.

Starting from a 3D CAD file (.stl file format), structure is built slice by slice from bottom to top, Fig. 2 left, in a vessel containing the photosensitive solution that crosslinks when irradiated by the projector 2D image (i.e., *layer by layer process*) thus potentially not restricting fabrication in height. Therefore, the main parameters involved in the printing process are slicing, layer exposure times and light absorber content in the liquid hydrogel (food colorant E133 that limits the penetration depth of the light) that ultimately contribute to the final z resolution of DLP structures, i.e. the minimum dimension of the features in z direction. To optimize definition and fidelity of the final 3D structures, slicing and irradiation values between 50 and 150 μm and 5 and 18 s per layer were tested, respectively, and E133 concentration was varied between 0.5 and 5% wt with respect to PulMA + PEGDA.

3D micrometric structures were achieved by 2PP using Nanoscribe GT Photonic Professional laser lithography system, equipped with an erbium-doped femtosecond laser source of ~150 mW at 780 nm, mounting a 63× 1.4 NA oil immersion objective (360 μm overall working distance). Drops of hydrogel solutions were deposited on methacrylated glass coverslips to improve adhesion of the fabricated features to the substrate [30]. A silicone gasket (approximatively 500–600 μm thick) with a second coverslip placed on top is used to contain the hydrogel and limit the evaporation rate of the solvent during the fabrication time. The laser beam is focused through the substrate into the photosensitive hydrogel; thus, the maximum structure height is of about 180–200 μm, limited by the objective working distance diminished by the substrate thickness (about 150 μm). The lateral size of the fabricated structures, instead, is determined, by the maximum scan range of the laser beam. In the Piezo-Scan-Mode used in our experiments, in which the laser is moved and the sample remains fixed, the scanned area is 300 μm^2, even though multiple blocks can be fabricated inside the maximum area of the gasket. A volumetric unit (voxel), having sub-micrometric dimensions, inside the hydrogel solution is selectively exposed by using a focalized pulsed laser light (Fig. 2 right). The beam is scanned in 3D by means of piezoelectric actuators in the x, y and z directions (*point by point process*), based on a computer-aided design (CAD), Fig. 3a.

A dose matrix was made for all the 3D shapes fabricated, necessary to characterize the material response toward TPP and identify the best 3D writing condition to induce the (meth)acrylic groups polymerization for each geometry (Fig. S5). Before cell seeding and characterization, initiators for SL and TPP were washed away in water overnight. The majority of E133 SL absorber was removed by frequently changing the water in the first days, but a faint blue color in the 3D printed scaffolds still persists even after 6 months of water immersion. Using the same procedure, DMSO was completely eliminated from the structures, as well.

2.5. Adhesion tests on 2D substrated with cell lines HEK 293

2D PulMA structures, with and without 30% PEGDA, were achieved by using a light source at 365 nm and crosslinking a 10% PulMA solution in a sandwich configuration, putting the solution between two coverslips, one of them functionalized with TMSPM to promote hydrogel adhesion.

Fibronectin (FN) functionalization was made putting a drop of FN solution (40 μg/ml) on top and let it be absorbed for 1.5 h.

HEK 293, 5000 cells/cm^2, were seeded on the substrates and after 24 h culturing the cells were fixed with PFA 4% and stained for nuclei with YOYO-1 Iodide. Bright field and epifluorescence images were taken with a Zeyss Axio Vert.A1.

2.6. Human MSC isolation and expansion

Bone marrow samples were obtained from orthopedic patients admitted to Pisa hospital for hip arthroplasty, after informed consent. During the surgical preparation of the medullary canal to house the prosthetic stem, the overflowing marrow blood (about 10–15 ml per person, depending on the prosthesis size) was collected [31]. The samples were treated anonymously and in accordance to the Helsinki declaration. The human MSC cultures were established as previously reported [32]. Briefly, the aspirate was diluted 1:3 in sterile saline, layered onto Ficoll as a density gradient and centrifuged at 400 ×*g* for 25 min. The mononuclear fraction was collected and seeded at a density of $0.2 \cdot 10^6$ cells/cm^2 on T-75 tissue culture flasks using DMEM-LG, supplemented with 10% FBS, 2 mM L-glutamine, 1% PEN-STREP solution and fluconazole. When 80% confluence was reached, the adherent cell layers were detached by using 0.25% trypsin and replated at a density of $1 \cdot 10^3$ cells/cm^2 for further expansion. Cell cultures were carried out in incubator under standard conditions, namely, 37 °C, 95% relative humidity, and 5% CO_2/95% air environment.

2.7. Culture of MSC/scaffold constructs

Pullulan-based scaffolds made by SL, cubes and stars, and TPL structures were sterilized by heating at 90 °C for 10 min in sterile double-distilled (dd)-H_2O followed by ultraviolet (UV) irradiation for 1 h and gentle washing with 3× PEN-STREP-fluconazole sterile saline solution. Human MSCs were detached with trypsin, counted under 0.2% Trypan Blue staining for viability evaluation and further seeding. SL stars ($n = 2$) and TPL structures ($n = 2$) printed on cover glasses were seeded with suspensions of 150,000 viable cells per sample in a sterile-filtered 2% w/v solution of gelatin in dd-H_2O. SL cubes ($n = 6$) were seeded with a suspension of 500,000 viable cells per scaffold in 50 μl of human pooled plasma added with $CaCl_2$ by using the clot method [33]. This method allows the rapid formation of a biodegradable and biocompatible loose fibrin gel which prevents cell loss during seeding, and is particularly useful in open-pore scaffolds as it gives sufficient time for cell/biomaterial attachment. After seeding, all the MSC/scaffold constructs were placed in the incubator for 1 h to favor cell adhesion

and finally fully covered with culture medium, at 6 ml/sample. The MSC/SL stars and MSC/TPL structures were cultured for 3 days, while the MSC/SL cubes were cultured up to 7 days.

2.8. Biological evaluation of MSC/PulMA structures

The SL star samples at different PEGDA concentrations were used to assess putative cytotoxic effects due to the material composition. At the endpoint, cell viability in the samples ($n = 1$) was investigated using the LIVE/DEAD® assay. Briefly, the culture medium was replaced with a staining solution consisting of 0.5 μl/ml Calcein AM and 2.0 μl/ml Ethidium homodimer-1 in sterile PBS. After 20 min incubation in the dark at 37 °C, the samples were observed under an inverted light microscope (Eclipse TI, Nikon, Amsterdam, The Netherlands) equipped for fluorescence analysis. Calcein AM stains in green the cells showing intracellular esterase activity (i.e., live cells), and Ethidium homodimer-1 in red the cells having lost cell membrane integrity (i.e., died or dying cells). For each sample, representative pictures at 5× magnification, including transmission field, were taken, under FITC and TRITC filters. Green and red channels of the micrographs were finally merged using Image-J software (version 1.46r).

The residual SL star samples ($n = 1$) were processed for fluorescence staining. Briefly, they were fixed in 4% (w/v) neutral buffered formalin diluted in 1× PBS at 4 °C overnight, washed twice in dd-H_2O for 5 min and in 1× PBS for 5 min, and finally incubated with a green-fluorescent phalloidin at room temperature in the dark for 3 h. After washing three times with 1× PBS for 5 min, the specimens were incubated with 10 μg/ml DAPI diluted in 1× PBS at room temperature in the dark for 10 min, then washed in 1× PBS for 5 min and observed under an inverted microscope (Nikon Eclipse Ti) equipped with a digital camera, FITC and DAPI filters at 40× magnification. Green and blue channels micrographs were finally merged as above.

The TPL structures ($n = 2$) were cultured with MSCs for 3 days, fixed, stained for fluorescence and observed as described above. Green and blue channel images were taken at 20×, 30× and 60× magnifications and merged as above.

The alamarBlue® (AB) assay was performed to monitor cell metabolic activity on MSCs seeded on SL cubes. This bioassay incorporates a REDOX indicator resulting in color change of the CM according to cell metabolism and can be performed multiple times on the same samples due to its negligible toxicity. MSC/SL cube constructs were placed on 24-well plates and AB assay was performed at 24 h, 48 h and 72 h time points after cell seeding. At each time-point, the samples ($n = 3$) and the negative controls ($n = 3$) were incubated for 3 h with culture medium containing the dye solution diluted according to the manufacturer's recommendations. After each assay, the supernatants were removed from the cultures and replaced with fresh culture medium. The absorbance (λ) of supernatants was measured with a spectrophotometer (Victor 3; PerkinElmer, Waltham, MA, USA) under a double wavelength reading (570 and 600 nm). Finally, the dye reduction percentage was calculated by correlating the absorbance values and the molar extinction coefficients of the dye at the selected wavelengths, following the equation provided by the manufacturer's protocol, and was given as a ratio between treated samples and controls. At the endpoint, the cell/SL cube constructs ($n = 2$) were fixed in 4% (w/v) neutral buffered formalin diluted in 1× PBS at 4 °C overnight. One construct was kept in culture for 1 week and AB assay was performed to check longer term cell metabolic activity.

The fixed MSC/SL cubes were processed for histology. Briefly, the samples were washed in 1× PBS, embedded in cryostatic medium at −80 °C (culture medium supplemented with 10% DMSO), fully sectioned with a standard cryo-microtome and the sections were mounted on glass slides, one every 30 μm, in order to evaluate scaffold colonization and cell/material interactions. Hematoxylin and eosin (H&E) staining was performed on the cryo-sections to reveal presence and morphology of MSCs in the constructs. After washings in dd-H_2O, the samples were incubated with hematoxylin for 5 min and washed in tap water for 5 min to reveal the staining. Subsequently, the specimens were incubated with eosin for 1 min, washed in dd-H_2O and mounted in the aqueous mounting medium. The stained sections were observed under a direct light microscope (Nikon Eclipse Ci, Amsterdam, The Netherlands) equipped with a digital camera. Additional cryo-sections were used for fluorescence staining. Briefly, the samples were washed twice in dd-H_2O for 5 min and in 1× PBS for 5 min, incubated with a phalloidin solution prepared according to manufacturer's instructions. After washing three times in 1× PBS for 5 min, the samples were incubated with 10 μg/ml DAPI, as described above. The sections were mounted in the aqueous mounting medium and observed at 20× magnification under an inverted microscope (Nikon Eclipse Ti) equipped with a digital camera, FITC and DAPI filters.

The LIVE/DEAD® cell viability assay and the ApoAlert® Annexin V apoptosis assay were performed on MSC/SL cubes ($n = 1$) following the manufacturers' procedure. Briefly, at the endpoint, the culture medium of each MSC/SL cube was replaced with a specific staining solution consisting of 0.5 μl/ml Calcein AM and 2.0 μl/ml Ethidium homodimer-1 in sterile PBS for viability assay, or 25 μl/ml Annexin V and 10 μl/ml Propidium Iodide in 1× binding buffer for apoptosis assay. After 20 min incubation in the dark at 37 °C, the samples were observed under an inverted light microscope (Eclipse TI, Nikon, Amsterdam, The Netherlands) equipped for fluorescence analysis, FITC, TRITC and DAPI filters. Calcein AM stains in green live cells showing intracellular esterase activity, and Ethidium homodimer-1 in red died or dying cells which had lost cell membrane integrity. On the other hand, Annexin V stains in green phosphatidylserine located at the cell membrane, which is a hallmark of apoptosis or programmed cell death, while Propidium Iodide in red cells having lost cell membrane integrity. For each sample, representative pictures 10× magnification were taken. Green and red channels of the micrographs were finally merged using Image-J software. After performing the apoptosis assay, the sample was fixed in 4% (w/v) neutral buffered formalin diluted in 1× PBS at 4 °C overnight, washed and incubated with 10 μg/ml DAPI diluted in 1× PBS, for 30 min at room temperature in the dark, then washed in 1× PBS for 5 min and observed under fluorescence microscopy to detect intact cell nuclei.

2.9. Statistical analysis

Quantitative data of alamarBlue® assay were presented as descriptive (mean ± standard deviation) and inferential statistics (p-values). Statistical significance was evaluated using the two-tailed paired t-test, followed by Bonferroni-Holm correction.

3. Results and discussion

3.1. Hydrogel formulation

To shape pullulan hydrogels in 3D, we first covalently linked methacrylated polymerizable units to the polysaccharide backbone (Fig. 1 and see legend). SL and TPL printing protocols entail the use of photopolymerization reactions. We used different radical photoinitiators: IRGACURE 819, whose absorption tail above 400 nm allows SL 3D printing (Fig. 2a), and P2CK as photoinitiator for TPL [23], with a broad two photon absorption range around 800 nm (see Methods on crosslinking conditions).

Since MA groups bound to pullulan (Fig. 1) are sterically hindered and thus poorly reactive, we decided to improve crosslinking efficiency by adding the bifunctional acrylate PEGDA to the photosensitive formulation. A further benefit of such addition, is to allow the tailoring of mechanical properties of the crosslinked PulMA hydrogel.

3.2. 3D fabrication by SL and TPL

Next, we aimed to carry out microfabrication on these substrates. Very few examples of 3D fabrication with SL can be found in literature

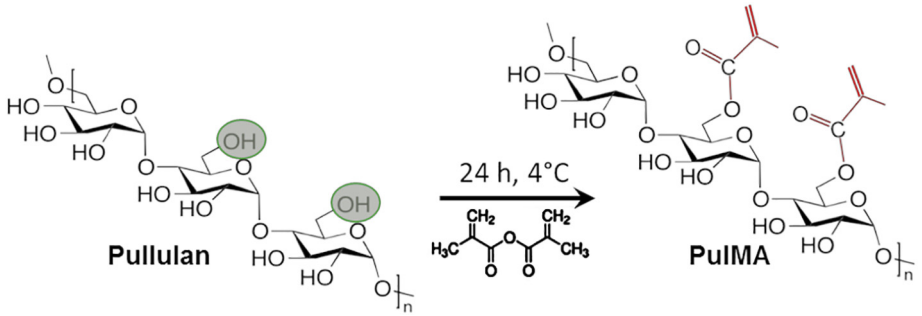

Fig. 1. Methacrylated pullulan (PulMA) synthesis reaction. A photosensitive and chemically crosslinkable polysaccharide is achieved through the introduction of unsaturated moieties covalently linked to the polysaccharide backbone. A functionalization degree of 3.8% was obtained by the addition of methacrylate that gives esterification reaction with free hydroxyl moieties mainly in C6 position (see Fig. S1).

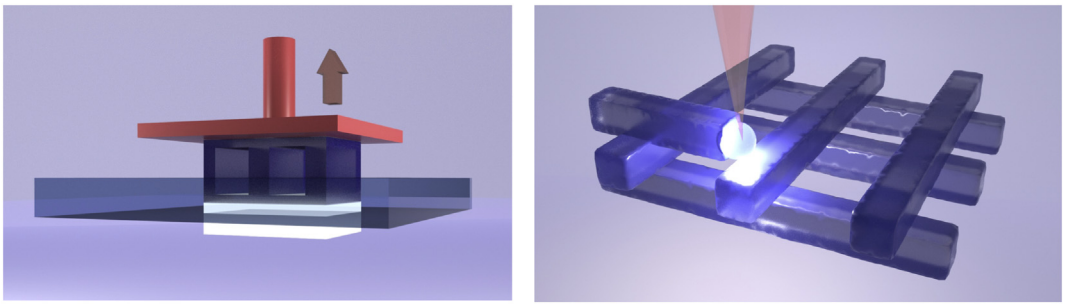

Fig. 2. Scheme of the SL fabrication system (left) and of TPL (right), in which the structure is built slice by slice from bottom to top or using a focalized pulsed laser light scanned in 3D respectively.

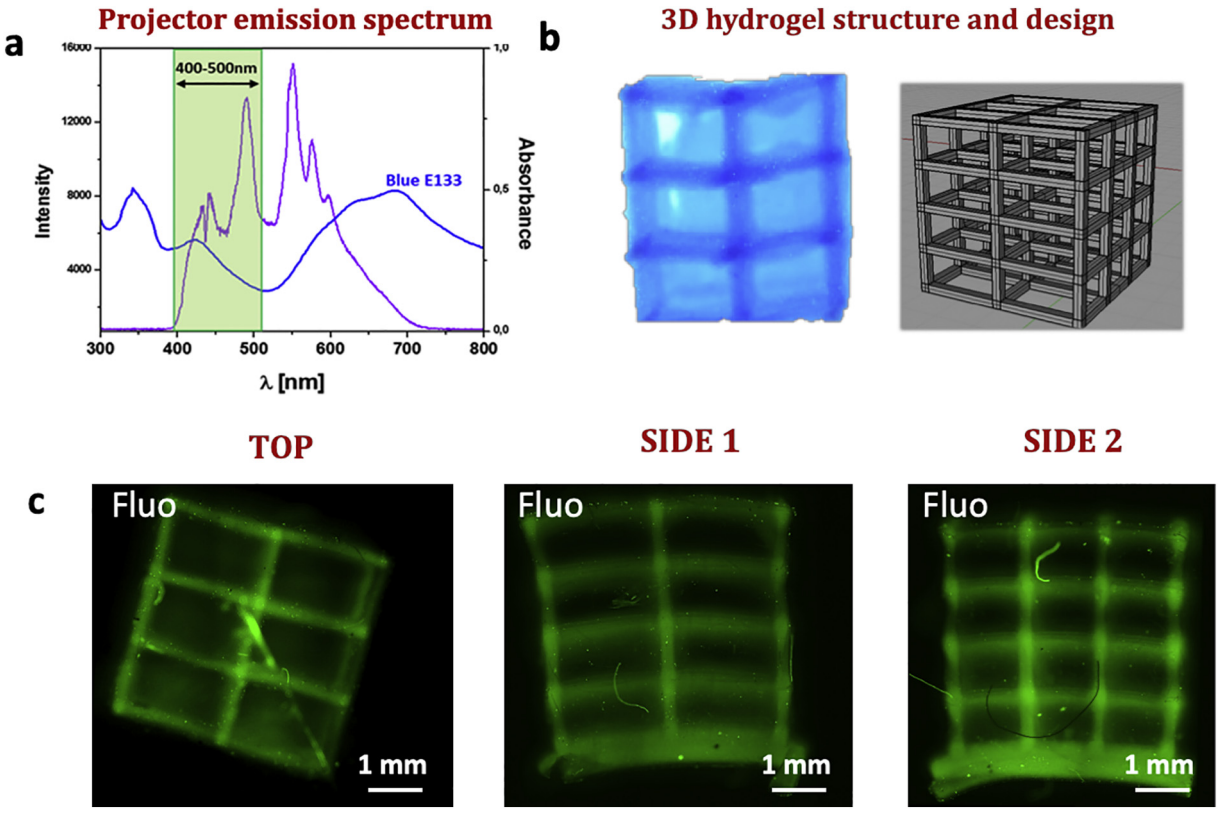

Fig. 3. Hydrogel fabrication by SL. a) The graph compares the emission spectrum of SL light source, the UV–visible spectrum of food colorant E133 used as light absorber and the wavelength range selected by the optical filter and actually used to exposed the photosensitive hydrogel. The latter is highlighted with the green rectangular. Optimization of the absorber concentration is shown in Fig. S2. b) Picture of a 3D structure (4.2 mm tall) fabricated by using PulMA with 30% PEGDA and a visible light 3D printer (slicing 50 μm, exposure time 12 s). In the inset, the 3D CAD model of the porous cube is reported. c) Fluorescence images of all cube perspectives (top, side1 and side2). The CAD design with the respective dimensions is shown.

[24] showing z-resolution, i.e., real structuring in the vertical direction of light projection. And the possibility to shape pullulan through TPL has not yet explored so far.

SL methodologies are known to require that resin cross-links layer-by-layer using projection optics that allows spatially controlled irradiation, according to a predefined CAD design [25] (Fig. 2 left). A defined 3D patterns is typically created thanks to an upward vertical movement of the sample in an ordered succession, layer by layer, of photocuring. However, this requires the presence of an absorber, to limit light penetration in vertical direction (allowing z-resolution).

We thus added to the hydrogel formulation a light absorber, with an absorption matching the emission range of the projector light source (Fig. 3a), to avoid overexposure of already printed layers. In this way, the radiation is confined in a small thickness of the photosensitive hydrogel liquid attached to the bottom part of the resin and the radical polymerization is promoted only in that thin layer, that results to be comparable with the set slicing parameter after optimization (Fig. S2). This protocol allows overcoming current limitations in vertical resolution of fabricated structures. Keeping in mind the potential biological applications of the printed structures, cell compatible food colorants were selected as light absorber, in particular Blue E133 (Fig. 3a). Fig. 3b shows, as example, a cube which edges are connected by suspended struts with nominal size of about 200 μm. The optical magnification of a strut clearly shows that the slice thickness is very close to the fixed slicing parameter (Fig. S3), confirming the effectiveness of food colorant strategy, allowing the fabrication with a minimal feature size of 50 μm.

We next asked if 3D fabrication of PulMA could be achieved at the micron scale by using TPL: for this, the crosslinking reaction is confined inside a small volume of photosensitive hydrogel, the voxel, where a specific laser power threshold is reached. The voxel is an ellipsoid generated by focusing an IR laser beam, that moving point by point in x, y and z directions builds the designed 3D microstructure [26,27] (Fig. 2b right).

From its dimension, that in the best cases is around 200 nm width and <1 μm height, depends the maximum resolution achievable. As shown by the fluorescence images in Fig. 4, woodpile patterns were successfully achieved with minimum dimension of 5 μm (Fig. 4a); perfect bulky circles with good reproducibility and stability were also fabricated (Fig. 4b), with a TPL process 3-times shorter if a shell&scaffold mode is used (Fig. S4). To exploit the peculiar technique resolution, complex cylindrical hollow structures with a honeycomb wall were fabricated: in this case the less bulky hollow framework of the thin wall undergoes to visible swelling toward the less constrained top part of the structure, as shown by the cross-section images (Fig. 4c). The behaviour is different for the ladder type shape of Fig. 4d, in which the rods guarantee a stability. To the best of our knowledge, this represents the first example of PulMA 3D structures generated by TPL.

3.3. Mechanical properties and cell culture

Next, we tested the mechanical properties and water absorption behaviour in SL printed samples (Figs. 5 and 6). To module these properties we opted for PulMA formulation with doses of the bifunctional crosslinker, PEGDA, allowing to increase or decrease covalent crosslinks density. We found that the elastic modulus and water absorption percentage increases and decreases respectively with increasing the PEGDA content, confirming that it contributes to the formation of a more crosslinked network.

However, the impact of PEGDA concentration is much larger on water absorption behaviour, causing an increasing of absorption from 50 to 400% in spite of an elastic modulus maintained between values of 2.5 and 1.5 kPa. Exposure time, shape and absorbance concentration did have impact on water absorption behaviour (Fig. 6a and b).

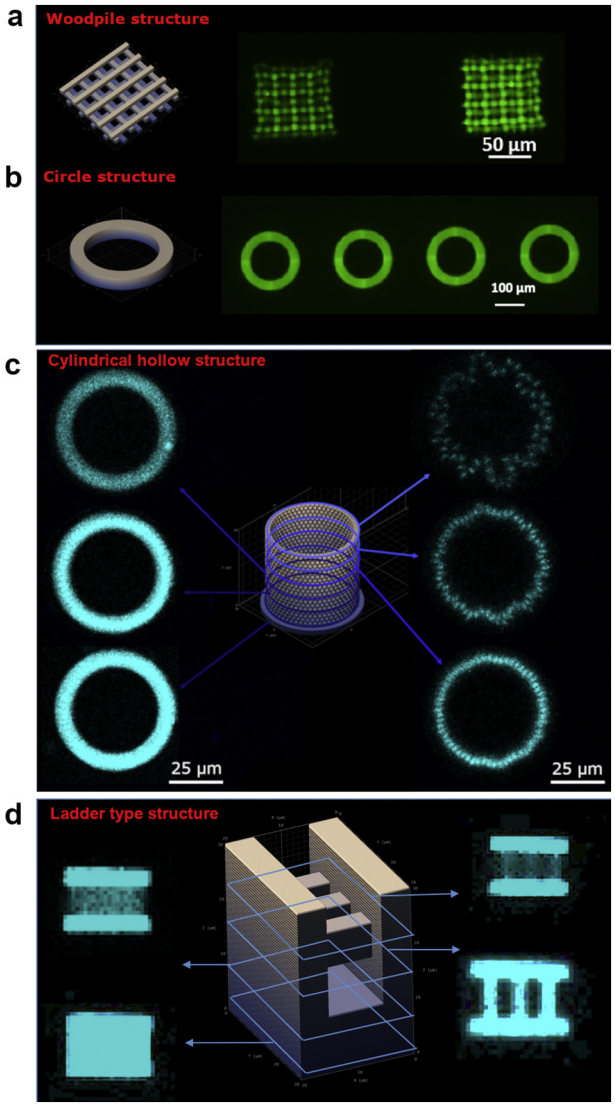

Fig. 4. Hydrogel structures fabricated in PulMA with 30% PEGDA by TPL: 3D CAD models and fluorescent images of a) woodpile like structures (rod dimensions 5 μm × 5 μm × 90 μm, height 50 μm), b) circle structures (outer diameter 150 μm, inner diameter 110 μm, height 20 μm), c) a cylindrical hollow scaffold with a honeycomb wall structure. In c and b z-sections of the structures are shown. Microscope magnification 20×, d) ladder type structures (28 μm × 20 μm, height 30 μm).

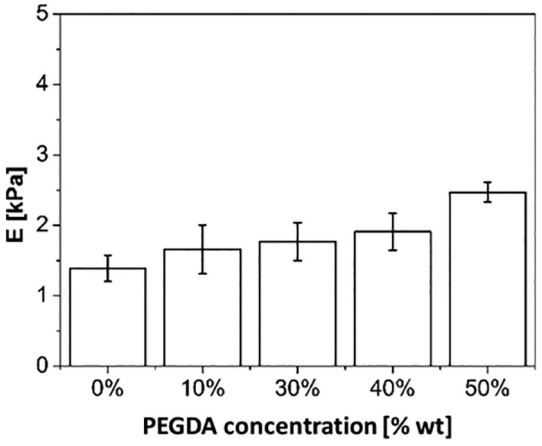

Fig. 5. Elastic modulus of PulMA hydrogels as function of PEGDA crosslinker concentration, crosslinked using 10 s exposure and 5% absorber. We believe that these crosslinking conditions resemble the exposure range used to fabricate 3D scaffold by SL, while for TPL the comparison is more complex.

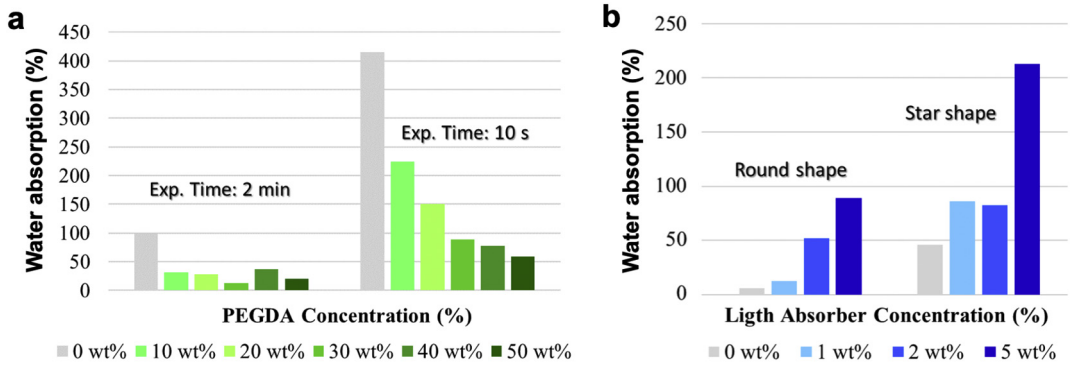

Fig. 6. Water absorption behaviour of PulMA hydrogels with a) increasing crosslinker concentration or b) different amount of food colorant as light absorber. Fixed PEGDA amount and exposure time were used (30% wt and 10 s, respectively). All measurements were performed in duplicate. The effect of exposure time and shape is also shown. Incomplete crosslinking determines higher water absorption when higher food colorant concentration or low doses are used (a). The effect of shape is also relevant, as shapes presenting a large superficial area (ex stars in b) showed a double tendency to swell respect to simple round shapes.

We then sought to determine whether these scaffolds could be used as biomaterials supporting the adhesion and expansion of mammalian cells. Indeed, the possibility to shape pullulan at different scales opens the possibility to pattern mechanical forces at the mesoscale, that has been recently shown to inform and mould the folding trajectories of epithelial cells [28]. Hydrolytic stability was preliminarily tested (Fig. S6). To impart adhesive properties, we functionalized 2D layers of pullulan with the adhesive extracellular matrix Fibronectin (FN). HEK293 cells indeed adhered on PulMA-PEGDA-FN, but not to PulMA and PulMA-PEGDA alone or PulMA-FN in absence of PEDGA crosslinking. Our interpretation of the latter data is that pullulan is by itself unable to associate with proteins, as such preventing FN coating in absence of PEGDA (Fig. 7).

Moving from 2D to 3D features, we next tested the potential of PulMA-PEGDA to serve as scaffold for Mesenchymal Stem Cells (MSCs). Also these cells don't adhere to PulMA-PEGDA alone (Figs. S7, S8, S9). These types of cells adhere strongly to fibrin, and, to this end, MSCs were mixed with human pooled plasma and seeded on SL 3D scaffolds. As shown in Fig. 8C–D, histological analysis confirmed the presence of cells attached to the PulMA surface, forming cell layers with well-organized f-actin microfilaments. Testing viability by alamarBlue® assay we found that MSCs were viable and metabolically active (Figs. 8A and S10).

4. Conclusions

In conclusion, 3D fabrication of PulMa structures with feature dimensions ranging from millimeters to microns was successfully demonstrated by using two light assisted 3D printing technologies, visible stereolithography, SL, and infrared Two-Photon Lithography, TPL. A pilot investigation on the cell response toward PulMA scaffolds was performed using HEK293 and human MSC cultures. PulMa substrates showed good cellular viability both on 2D and 3D patterns, showing cellular adhesion only in presence of fibronectin or fibrin functionalization on millimetric 3D structures.

As the integration of multi-scale patterns in the same structure can be an important step forward in tissue engineering and regenerative medicine fields and hydrogel fabrication with these two different scale sizes and technologies have not commonly reported, this study confirms PulMA hydrogels as excellent substrates supporting cell culture after proper functionalization, with endowed mechanical properties and 3D printing feature sizes. On the other hand, the non-adhesive property of PulMA could allow to fine tuning of adhesive areas and patterning of individual cells and of monolayers in both 2D and 3D, giving vast opportunities for cell engineering through microfabrication. In future, fabrication by SL and TPL in presence of pre-embedded cells is potentially feasible with PulMA

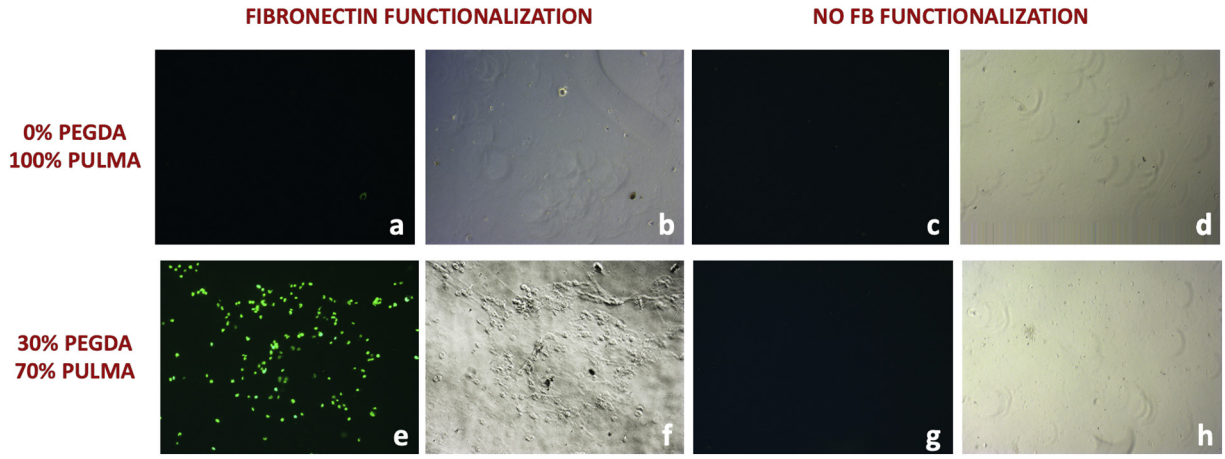

Fig. 7. cell line (HEK293) cultured on 2D substrates of PulMA with 0 (a–d) or 30% (e–h) PEGDA, with (a, b, e, f) and without (c, d, g, h) fibronectin functionalization. Hydrogels without fibronectin functionalization never support cell-adhesion (c, d, g, h) while only in presence of PEGDA the protein functionalization is effective for cell adhesion (e). These results indicate a poor absorption of fibronectin on pure PulMA and confirm that PulMA has strong repellence against both cells and proteins but is biocompatible and can be easily functionalized with proteins, allowing cell adhesion.

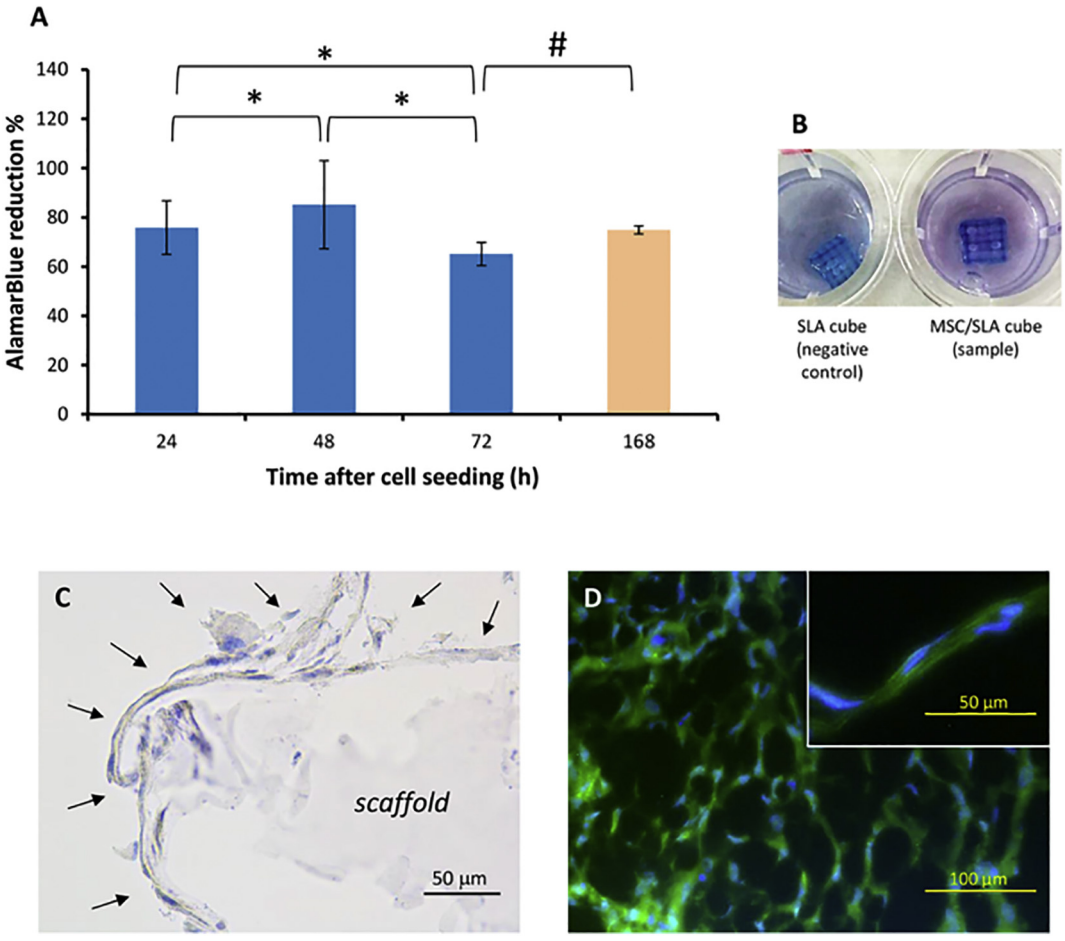

Fig. 8. Results of MSCs cultured on PulMA 3D SL cubes. (A, B) AlamarBlue® assay showing cell metabolic activity: (A) Bar graph showing a metabolic activity trend of MSCs seeded inside the scaffolds over time. The experiment focused on the first 3 days to corroborate other findings. One sample was maintained in culture for 7 days to assess long term conditions. Statistical significance: $^{*}p < 0.05$, $^{\#}p = 0.016$, the latter to be considered with a qualitative value. (B) Test results are visible as culture medium change, turning from blue to pink. (C, D) Results of histologic analysis performed on cryo-sections of MSC/SL cube constructs at 3 days after seeding: (C) H&E staining showing that human MSCs adhered onto the scaffold surface; scale bar is 50 µm, and (D) F-actin and DAPI staining showing cell colonization of the scaffold; scale bar is 100 µm. Lens shows MSCs expressing well-structured f-actin microfilaments; scale bar is 50 µm.

at no or low toxicity given the use of visible and infrared radiation, respectively. This paper sets the foundation for future studies, aiming at investigating whether a particular recognition of the scaffold microstructures, stiffness or swelling degree could be used to drive cell fate and behaviour or to organize complex tissues (e.g., orientation of myotubes, or tissue-like architectures).

Authors contributions

G. Della Giustina, A. GDG and AG contributed with pullulan synthesis and fabrication. TP and SG carried out cell adhesion and bioassays. LB contributed to two-photon fabrication. PS made NMR analyses. DD, LT and SD contributed with MSC experiments. GB conceived and supervised this work, and write the manuscript.

Acknowledgements

This work is supported by a University of Padova SID grant and MIUR-FARE grant to G.B., and by a Foundation Cariparo Starting grant to T.P. G.B. acknowledges Prof. Robert Liska and Dr. Maximilian Tromayer of the Institute of Applied Synthetic Chemistry, Vienna University of Technology, for providing the P2CK 2Photon photoinitiator. S.D., L.T. and D.D. gratefully acknowledge Tuscany Region (CUCCS 2014 project) for funding stem cell research.

Data availability

All relevant data are included in the manuscript as Source Data or Supplementary information; all other data are available from the corresponding authors upon reasonable request.

Appendix A. Supplementary data

Supplementary data to this article can be found online at https://doi.org/10.1016/j.matdes.2018.107566.

References

[1] S.W. Crowder, V. Leonardo, T. Whittaker, P. Papathanasiou, M.M. Stevens, Cell Stem Cell 18 (2016) 39–52.
[2] M.W. Tibbitt, K.S. Anseth, Biotechnol. Bioeng. 103 (2009) 655–663, https://doi.org/10.1002/bit.22361.
[3] N. Annabi, J.W. Nichol, X. Zhong, C. Ji, S. Koshy, A. Khademhosseini, F. Dehghani, Tissue Eng. B 16 (2010) 371.
[4] C.-C. Lin, C.S. Ki, H. Shih, J. Appl. Polym. Sci. 132 (2015), 41563. .
[5] J. Malda, et al., Engineering hydrogels for biofabrication, Adv. Mater. 25 (2013) 5011–5028.
[6] S.K. Seidlits, C.E. Schmidt, J.B. Shear, Adv. Funct. Mater. 19 (2009) 1–9.
[7] L.G. Bracaglia, B.T. Smith, E. Watson, N. Arumugasaamy, A.G. Mikos, J.P. Fisher, Acta Biomater. 56 (2017) 3–13.
[8] L. Brigo, A. Urciuolo, S. Giulitti, G. Della Giustina, M. Tromayer, R. Liska, N. Elvassore, G. Brusatin, Acta Biomater. 55 (2017) 373–384.

[9] J. Bauer, A. Schroer, R. Schwaiger, O. Kraft, Nat. Mater. 15 (2016) 438–443.
[10] L. Montemayor, V. Chernow, J.R. Greer, MRS Bull. 40 (2015) 1122.
[11] R.S. Singh, N. Kaur, V. Rana, J.F. Kennedy, Carbohydr. Polym. 171 (2017) 102–112.
[12] a) V.D. Prajapati, G.K. Jani, S.M. Khanda. 2013 95 540–549.
b) R. Nakahashi-Ouchid, Y. Yuki, H. Kiyono, Expert Rev. Vaccines 16 (12) (2017) 1231.
[13] S. Bang, E. Lee, Y.G. Ko, W.I. Kim, O.H. Kwon, Int. J. Biol. Macromol. 87 (2016) 155–162.
[14] L. Suguna, J. Clin. Exp. Dermatol. Res. 5 (2014) 63.
[15] K.R. Sugumarana, V. Ponnusamib, Review on production, downstream processing and characterizationof microbial pullulan, Carbohydr. Polym. 173 (2017) 573–591.
[16] P. Shao, B. Niu, H. Chen, P. Sun, Int. J. Biol. Macromol. (17) (2017) 33072–33076 (S0141-8130).
[17] R.S. Singh, N. Kaur, V. Rana, J.F. Kennedy, Carbohydr. Polym. 153 (2016) 455–462.
[18] R.K. Upadhyay, Adv. Tissue Eng. Regen. Med. 2 (2) (2017) 145–151.
[19] M.F. Arnobit Cutiongco, M.H. Tan, M.Y. Kuang Ng, C. Le Visage, E.K.F. Yim, Acta Biomater. 10 (10) (2014) 4410–4418.
[20] Amrita, A. Arora, P. Sharma, D.S. Katti, Carbohydr. Polym. 123 (2015) 180–189.
[21] J.C. Fricain, S. Schlaubitz, C. Le Visage, I. Arnault, S.M. Derkaoui, R. Siadous, S. Catros, C. Lalande, R. Bareille, M. Renard, T. Fabre, S. Cornet, M. Durand, A. Léonard, N. Sahraoui, D. Letourneur, J. Amédée, Biomaterials (2013) 2947–2959.
[22] E. Zanchetta, M. Cattaldo, G. Franchin, M. Schwentenwein, J. Homa, G. Brusatin, P. Colombo, Adv. Mater. 28 (2016) 370–376.
[23] Z. Li, J. Torgersen, A. Ajami, S. Muhleder, X. Qin, W. Husinsky, W. Holnthoner, A. Ovsianikov, J. Stampfl, R. Liska, RSC Adv. 3 (2013) 15939–15946.
[24] K.C. Hribar, P. Soman, J. Warner, Peter Chung, S. Chen, Lab Chip 14 (2014) 268.
[25] P.W. Ferry Melchels, J. Feijen, D.W. Grijpma, Biomaterials 31 (2010) 6121–6130.
[26] J. Fischer, G. von Freymann, M. Wegener, Adv. Mater. 22 (2010) 3578–3582.
[27] C. Barner-Kowollik, M. Bastmeyer, E. Blasco, P. Mueller, G. Delaittre, B. Richter, M. Wegener, Angew. Chem. Int. Ed. 56 (2017).
[28] A.J. Hughes, H. Miyazaki, M.C. Coyle, J. Zhang, M.T. Laurie, D. Chu, Z. Vavrušová, R.A. Schneider, O.D. Klein, Z.J. Gartner, Dev. Cell 44 (2) (2018) 165–178.
[29] H. Bae, A.F. Ahari, H. Shin, J.W. Nichol, C.B. Hutson, M. Masaeli, S.-H. Kim, H. Aubin, S. Yamanlar, A. Khademhosseini, Soft Matter 7 (2011) 1903.
[30] G. Della Giustina, S. Giulitti, L. Brigo, M. Zanatta, M. Tromayer, R. Liska, N. Elvassore, G. Brusatin, Macromol. Rapid Commun. 38 (2017), 1600570. .
[31] L. Trombi, S. Danti, S. Savelli, S. Moscato, D. D'Alessandro, C. Ricci, S. Giannotti, M. Petrini, J. Vis. Exp. 118 (2016) 54845, https://doi.org/10.3791/54845.
[32] L. Trombi, L. Matti, S. Pacini, D. D'Alessandro, B. Battolla, E. Orciuolo, G. Buda, R. Fazzi, S. Galimberti, M. Petrini, J. Orthop. Res. 26 (2008) 176–183.
[33] C. Mota, M. Labardi, L. Trombi, L. Astolfi, M. D'Acunto, D. Puppi, G. Gallone, F. Chiellini, S. Berrettini, L. Bruschini, S. Danti, Mater. Des. 122 (2017) 206–219.